DARPA ORDER 9526

ENHANCED CERIA SOLID ELECTROLYTE FUEL CELL DEVELOPMENT

Reduction of Electronic Conductivity Permits use of a Solid Ceria Electrolyte in High Efficiency High Power Density Fuel Cells at Temperatures Compatible with Metallic Cell Hardware

Prepared by

D. L. Maricle

International Fuel Cells
P.O. Box 739
195 Governors Highway
South Windsor, CT 06074

January 1990

FCR-10815

Fifth Interim Report for Quarter Ending September, 1989

Contract Number N00014-88-C-0390

Prepared for

Defense Advanced Research Project Agency
1400 Wilson Blvd.
Arlington, VA 22209-2308

Office of Naval Research
800 North Quincy Street
Arlington, VA 2221

International Fuel Cells

P.O. Box 739
195 Governors Highway
South Windsor, Connecticut 06074

1/24/90 Fifth Interim, September 1989

ENHANCED CERIA SOLID ELECTROLYTE FUEL CELL DEVELOPMENT
Reduction Electronic Conductivity Permits use of a Solid Ceria Eelctrolyte in Hight Efficiency High Power Density Fuel Cells at Temperatures Compatible with Metallic Cell Hardware

D. L. Maricle

International Fuel Cells
P.O. Box 739
195 Governors Highway
South Windsor, CT 06074

Office of Naval Research
800 North Quincy Street - 11132
Arlington, VA 22217-5000

The high operating emperature of zirconia based solid oxide fuel cells has been shown in many studies to have advantages for both space and terrestrial applications. The high heat rejection temperature minimizes radiator soze and weight for high atmospheric and space applications. Mobileand stationary terrestrial application take advantage of a cell temperature high enough to directly reform hydrocarbon fuels, achieving high efficiency and energy density.

Cell voltage, Useful external current, Efficiency, Power density 40

Unclassified Unclassified Unclassified Unlimited

GENERAL INSTRUCTIONS FOR COMPLETING SF 298

The Report Documentation Page (RDP) is used in announcing and cataloging reports. It is important that this information be consistent with the rest of the report, particularly the cover and title page. Instructions for filling in each block of the form follow. It is important to **stay within the lines to meet optical scanning requirements.**

Block 1. Agency Use Only (Leave Blank)

Block 2. Report Date. Full publication date including day, month, and year, if available (e.g. 1 Jan 88). Must cite at least the year.

Block 3. Type of Report and Dates Covered. State whether report is interim, final, etc. If applicable, enter inclusive report dates (e.g. 10 Jun 87 - 30 Jun 88).

Block 4. Title and Subtitle. A title is taken from the part of the report that provides the most meaningful and complete information. When a report is prepared in more than one volume, repeat the primary title, add volume number, and include subtitle for the specific volume. On classified documents enter the title classification in parentheses.

Block 5. Funding Numbers. To include contract and grant numbers; may include program element number(s), project number(s), task number(s), and work unit number(s). Use the following labels:

C	- Contract	**PR**	- Project
G	- Grant	**TA**	- Task
PE	- Program Element	**WU**	- Work Unit Accession No.

Block 6. Author(s). Name(s) of person(s) responsible for writing the report, performing the research, or credited with the content of the report. If editor or compiler, this should follow the name(s).

Block 7. Performing Organization Name(s) and Address(es). Self-explanatory.

Block 8. Performing Organization Report Number. Enter the unique alphanumeric report number(s) assigned by the organization performing the report.

Block 9. Sponsoring/Monitoring Agency Names(s) and Address(es). Self-explanatory.

Block 10. Sponsoring/Monitoring Agency. Report Number. (If known)

Block 11. Supplementary Notes. Enter information not included elsewhere such as: Prepared in cooperation with...; Trans. of ..., To be published in .... When a report is revised, include a statement whether the new report supersedes or supplements the older report.

Block 12a. Distribution/Availablity Statement. Denote public availability or limitation. Cite any availability to the public. Enter additional limitations or special markings in all capitals (e.g. NOFORN, REL, ITAR)

DOD - See DoDD 5230.24, "Distribution Statements on Technical Documents."
DOE - See authorities
NASA - See Handbook NHB 2200.2.
NTIS - Leave blank.

Block 12b. Distribution Code.

DOD - DOD - Leave blank
DOE - DOE - Enter DOE distribution categories from the Standard Distribution for Unclassified Scientific and Technical Reports
NASA - NASA - Leave blank
NTIS - NTIS - Leave blank.

Block 13. Abstract. Include a brief (Maximum 200 words) factual summary of the most significant information contained in the report.

Block 14. Subject Terms. Keywords or phrases identifying major subjects in the report.

Block 15. Number of Pages. Enter the total number of pages.

Block 16. Price Code. Enter appropriate price code (NTIS only).

Blocks 17. - 19. Security Classifications. Self-explanatory. Enter U.S. Security Classification in accordance with U.S. Security Regulations (i.e., UNCLASSIFIED). If form contains classified information, stamp classification on the top and bottom of the page.

Block 20. Limitation of Abstract. This block must be completed to assign a limitation to the abstract. Enter either UL (unlimited) or SAR (same as report). An entry in this block is necessary if the abstract is to be limited. If blank, the abstract is assumed to be unlimited.

ENHANCED CERIA SOLID ELECTROLYTE FUEL CELL DEVELOPMENT

Reduction of Electronic Conductivity Permits use of a Solid Ceria Electrolyte in High Efficiency High Power Density Fuel Cells at Temperatures Compatible with Metallic Cell Hardware

Prepared by

D. L. Maricle

International Fuel Cells
P.O. Box 739
195 Governors Highway
South Windsor, CT 06074

January 1990

FCR-10815

Fifth Interim Report for Quarter Ending September, 1989

Contract Number N00014-88-C-0390

Prepared for

Defense Advanced Research Project Agency
1400 Wilson Blvd.
Arlington, VA 22209-2308

Office of Naval Research
800 North Quincy Street
Arlington, VA 22217

TABLE OF CONTENTS

LIST OF ILLUSTRATIONS

LIST OF TABLES

SUMMARY

The primary obstacle to the use of ceria as a high power density solid oxide fuel cell electrolyte has been a low level electronic short. This develops under reducing (anode) conditions as a result of partial reduction of the CeO_2 lattice. This results in a decrease in:

a) cell voltage,
b) useful external current,
c) efficiency,
d) power density.

A dopant concept has been shown to lower the anode PO_2 below which the short becomes detrimental (electrolytic domain boundary) by two orders of magnitude. Two dopants, A and B have been shown to be effective. The optimum A dopant level was determined.

Analysis of the activation energies for electronic and ionic conduction indicate that the dopant is effective in reducing the short by trapping the electronic charge carriers rather than preventing partial reduction of the ceria. Measurement of the grain boundary and bulk conductivities show the overall ionic conductivity is limited by grain boundary resistance. If lower grain boundary resistance can be achieved by processing changes, another two orders of magnitude improvement in electrolytic domain boundary is possible.

An attempt to limit the short by establishing an electronically resistive grain boundary barrier layer was abandoned. A separate grain boundary phase was difficult to maintain during the sinter densification step.

The dopant approach was selected for further development.

INTRODUCTION

The high operating temperature of zirconia based solid oxide fuel cells has been shown in many studies to have advantages for both space and terrestrial applications. The high heat rejection temperature minimizes radiator size and weight for high atmospheric and space applications. Mobile and stationary terrestrial applications take advantage of a cell temperature high enough to directly reform hydrocarbon fuels, achieving high efficiency and energy density.

Government funded solid oxide fuel cell (SOFC) efforts are concentrated on the monolithic and tubular cell designs employing zirconia as the oxide ion conduction membrane. Zirconia requires an operating temperature of 1000°C to achieve adequate electrolyte conductivity. All-ceramic cell structures are used in both cases, leading to fragile, failure prone cells, and manufacturing steps which are difficult to scale up and costly. IFC's molten carbonate fuel cell development demonstrates the reliability of ductile sheet metal parts used for gas flow fields, separator plates, and frames in the 650°C temperature range. Ceria doped with gadolinia has ionic conductivity at 700°C comparable to zirconia at 1000°C. At 700°C a variety of stainless steels offer acceptable strength and oxidation resistance for use as cell hardware.

A critical issue must be resolved if ceria is to be an ideal fuel cell electrolyte. When exposed to the reducing atmosphere at the fuel side, it develops electronic as well as ionic conductivity. This contributes to loss of efficiency at low power levels. This program addressed two means of ameliorating this loss. They were:

1. Modifying the ceria electronic structure through doping to enhance the ionic and diminish the electronic conductivity.

2. Incorporating non-electronically conducting barrier layers at the ceria grain boundaries to block electron flow.

Additional description for the rational behind these approaches can be found in the First Interim Report for the Quarter Ending September, 1988, FCR-9983. During this report period both approaches were pursued, and an optimum composition selected for further development.

RESULTS

Task 1 Literature Search

Task 1 has been completed and is inactive.

Task 2 Experimental Evaluation of Dopants to Increase the Ratio of Ionic to Electronic Conductivity

2.1 Sample Preparation and Electrical Measurement Techniques

Samples were prepared from 99.999 percent oxides by the mixed oxide technique during this report period. This change to high purity oxides was made in an effort to ensure reproducible and accurate results. The materials were purchased from Cerac. While believed to be too costly for practical fuel cell application, high purity minimizes the chance of measuring spurious results due to tramp dopants.

Weighed quantities of the oxides were ground in an agate mortar and pestle, calcined at 1000°C for 18 hours, and then reground. Pellets were pressed at 3636 Kg in a 1.85 cm pellet press using 2 w/o DOW XUS 40303 experimental binder. Sintering was accomplished in a Theta Furnace at 1600°C for 12 - 24 hours in air. A heat up rate of 2^0/min and a cool down rate of 0.5^0/min were used to minimize cracking. Sintered sample thickness was of the order of 2.5 min.

Pt paste (Heraeus CL115100) contacts were applied and fired onto the faces of the sintered discs at 1000°C. Pt screen current collectors were attached with a second thin layer of Pt paste.

Samples were placed in an Inconel retort for electrical property measurements as a function of oxygen partial pressure and temperature. The retort was fitted with gas inlet and exit ports, thermocouple wells, and electrical feed through and heated in a Sola Basic Lindberg furnace. The high PO_2 gas environments were provided by mixtures of O_2, N_2, and CO_2. The low PO_2 environments were established with H_2 and $H_2 - N_2$ mixtures passed through a water saturator set at 25°C - 85°C. Measurements were taken at a high PO_2, (0.1 atm), then the lower PO_2s, and finally the high PO_2 was repeated to ensure no mechanical damage had occurred as a result of the partial reduction of the ceria. These experimental procedures led to stable, and reproducible data.

AC impedance analysis was used to separate electrode impedance from the impedance of the ceramic electrolyte. A Solatron 1250 Frequency Response Analyzer, and a 1286 electrochemical interface, both controlled by an IBM-XT computer with Z-Plot™ software was used to obtain the impedance spectra. At 700°C, the usual measurement temperature, the complex plane impedance plot generally showed the intersection of the low impedance end of the electrode impedance arc with the real axis. See for example Figure 1 taken from reference 4. This value was taken as the overall electrolyte impedance. Volume conductivity was calculated as usual from the geometric factors and corrected for porosity by the Bruggeman equation using a power of 1.5(1). At lower temperatures electrolyte bulk and grain boundary impedances could also be measured. At the lowest PO_2 levels the ionic impedance was essentially shorted by the electronic conduction and only a single point plot resulted.

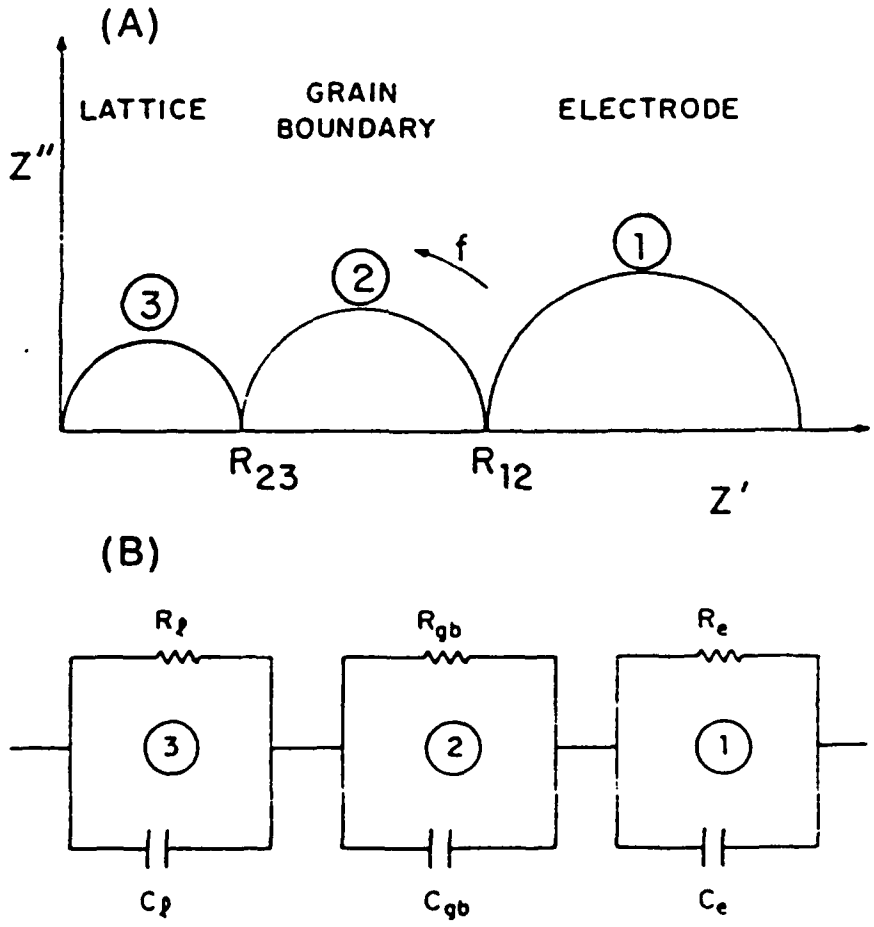

Figure 1. (A) Schematic diagram of a complex impedance plot showing arcs due to three processes. The arrow indicates the direction of increasing frequency. (B) The equivalent circuit that gives rise to the three arcs shown in (A).

2.2 Verification of Improved Electrolytic Domain Boundary by AC Impedance Analysis

Improvement in the level of electronic shorting induced in the ceria electrolyte under anode (reducing) conditions was assessed by measuring the electrolytic domain boundary (EDB). The EDB was determined by measuring the electrolyte impedance under gas compositions with a PO_2 ranging from 10^{-1} to 10^{-24} atm at 700°C as described in Section 2.1. The value of the volume conductivity calculated from the $PO_2 = 10^{-1}$ atm data was assumed to be the ionic conductivity. The increase in volume conductivity observed as the PO_2 was lowered was taken as the electronic conductivity. This allowed calculation of the electronic conductivity at any PO_2 simply by subtracting the ionic conductivity from any increase in conductivity observed at low PO_2 (2).

The improved experimental techniques described in Section 2.1 were used in order to verify the lower EDB results reported during the last report period for the modified compositions. Steady reproducible conductivity measurements resulted. A sample of $Ce_{0.8}Gd_{0.2}O_{2-Y}$ was measured with the improved techniques as a reference point, and for comparison to EDB values from the literature for the same composition(3).

Figure 2 illustrates the impact of A doping on the total conductivity of the doped ceria electrolytes at 700°C. Based on this work, the ionic conductivity is enhanced, while the electronic conductivity is depressed. The net result is a reduction in the EDB of 2 orders of magnitude. This is illustrated in Table I. Measurements on each of two samples with and without 1 atom percent A dopant are compared with results calculated from data of Kudo and Obayashi(3) for Gd doped ceria. In this and following tables σ_{ion} refers to the ionic conductivity, σ_{el} to the electronic conductivity, and EDB to the electrolytic domain boundary.

TABLE I
ELECTRICAL PROPERTIES OF DOPED CERIA ELECTROLYTES AT 700°C

Composition	σion $PO_2 = 0.1$ (S/cm)	σel $PO_2 = 10^{-23}$ (S/cm)	EDB (atm)
Ce0.8Gd0.2O2-Y - This study	2.8×10^{-2}	4.7×10^{-1}	3.5×10^{-19}
Ce0.8Gd0.2O2-Y - This study	1.4×10^{-2}	1.8×10^{-1}	1.3×10^{-19}
Ce0.8Gd0.2O2-Y - Ref (3)	4.7×10^{-2}	4.6×10^{-1}	1.24×10^{-19}
Oxide B1	3.7×10^{-2}	1.9×10^{-1}	4.6×10^{-21}
Oxide B1	4.2×10^{-2}	2.6×10^{-1}	4.7×10^{-21}

The reduction in EDB accomplished by Dopant A is consistent and reproducible. The value of the ionic conductivity of Gd doped ceria is lower in this work then Kudo and Obayashi(3). This may reflect a different micro-structure or level of impurities.

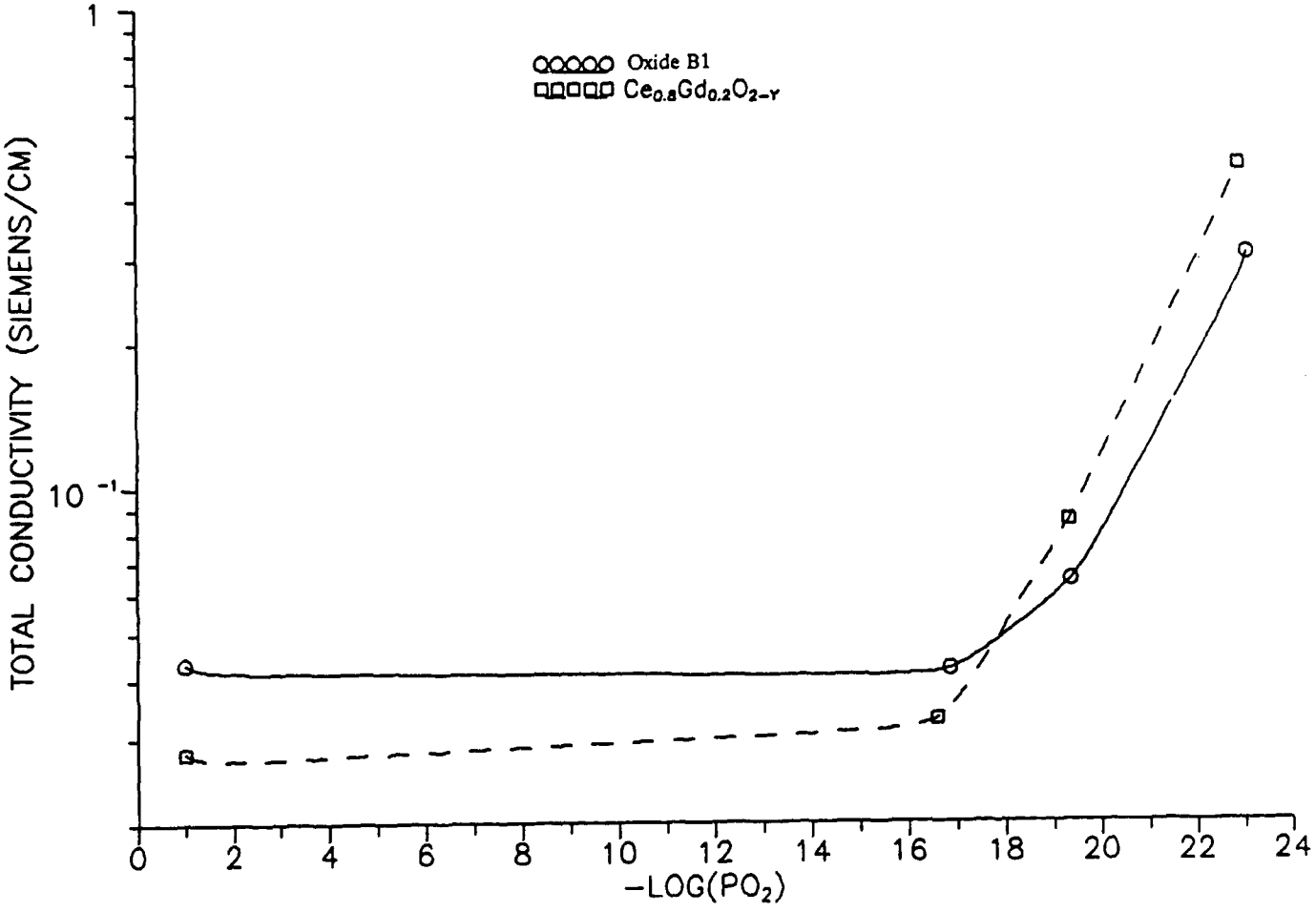

Figure 2. Total Conductivity as a Function of Oxygen Partial Pressure 700°C

2.3 Optimization of Composition

The one metal atom percent Dopant A level used initially was selected on the basis of work reported previously which showed no benefit at the 5 to 20 percent level. However it is necessary to determine the optimum level for the dopant. This was done by varying the A level over the range of .01 to 6 metal atom percent. The compositions tested were: Oxides B4, B1, B3, and B6. The EDBs and the electronic conductivity at a PO_2 of 10^{-23} and 700°C are shown in Figures 3 and 4. Both reach a broad minimum in the 1 - 3 metal atom percent range. This is the optimum composition for these dopants, and the data shown in Section 2.2 represents near optimum electrical properties for these materials.

Table II shows the conductivity data obtained on these materials in tabular form. It is clear that the A level has no impact on the ionic conductivity over the range of compositions studied. This suggests that the low ionic conductivity reported in Section 2.2 for $Ce_{0.8}Gd_{0.2}O_{2-Y}$ in this study relative to Kudo and Obayashi(3) was likely due to poor micro-structure, and that the effect of the A dopant is primarily to lower the electronic conductivity.

TABLE II
ELECTRONIC PROPERTIES OF DOPED CERIA
EFFECT OF DOPANT LEVEL
700°C

Composition	Dopant Level (metal atom%)	σion $PO_2 = 0.1$ (S/cm)	σel $PO_2 = 10^{-2}$ (S/cm)	EDB (atm)
Oxide B4	0.1	4.2×10^{-2}	2.7×10^{-1}	7.5×10^{-21}
Oxide B1	1.0	3.7×10^{-2}	1.9×10^{-1}	4.6×10^{-21}
Oxide B3	3.0	4.3×10^{-2}	2.0×10^{-1}	1.1×10^{-21}
Oxide B6	6.0	3.5×10^{-2}	2.3×10^{-1}	3.5×10^{-21}

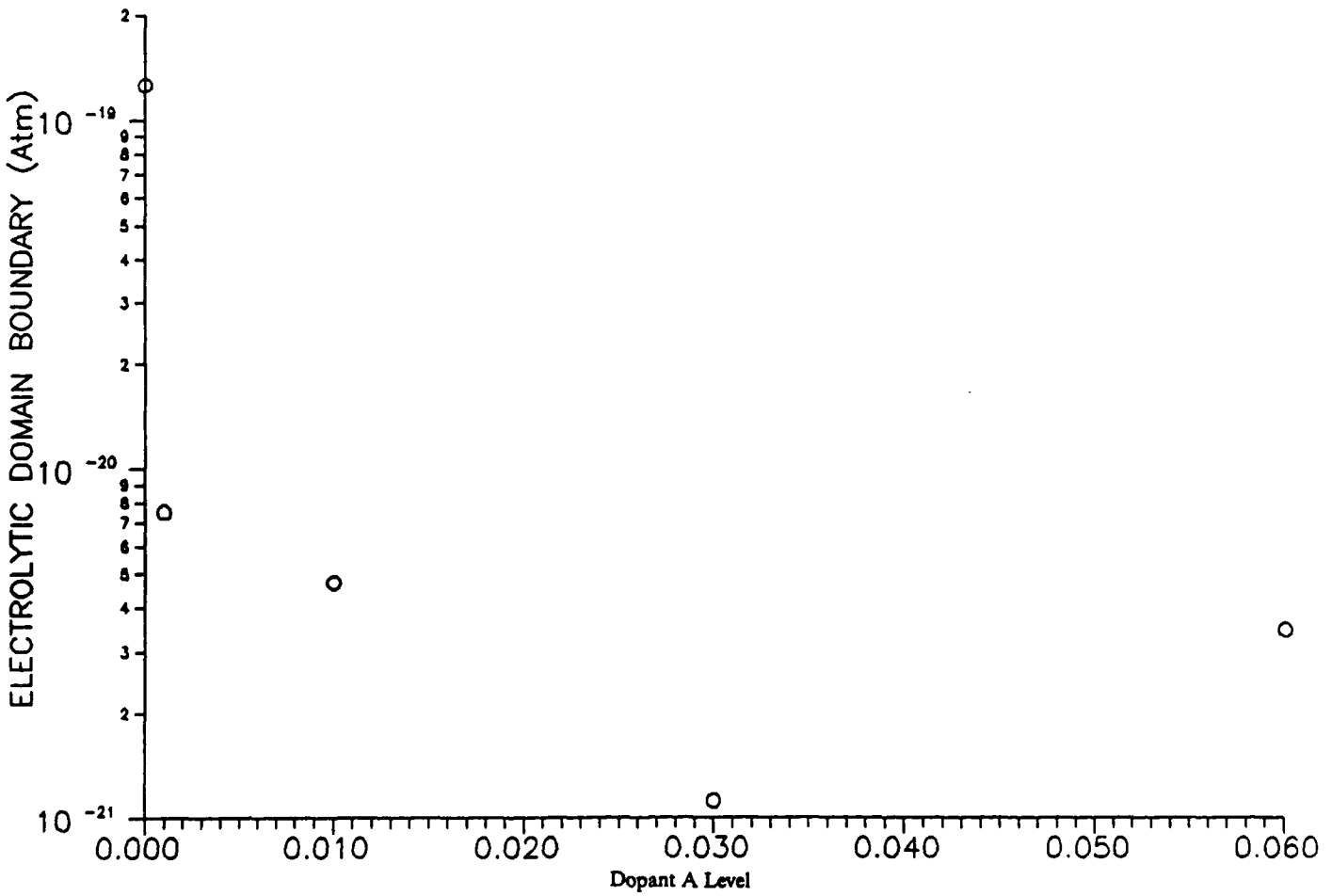

Figure 3. Electrolytic Domain Boundary Vs. Dopant A Level at 700°C

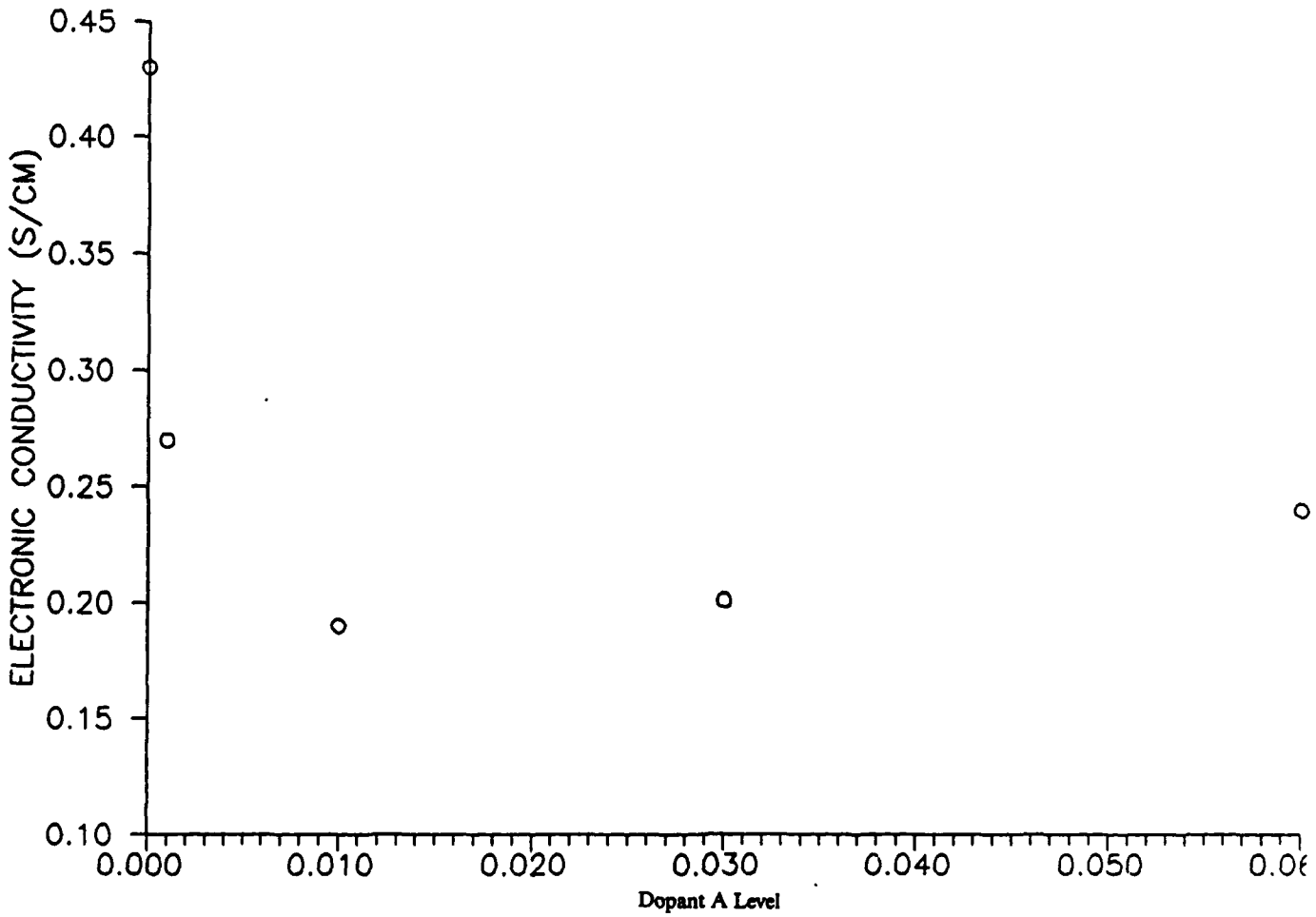

Figure 4. Electronic Conductivity at $PO_2 = 10^{-23}$ Vs. Dopant A Level

2.4 Measurement of Activation Energy of Electronic and Ionic Conductivity

Measurement of the behavior of electronic and ionic conductivity as a function of temperature was undertaken for two important reasons, one practical and one theoretical. No high power density fuel cell can be operated as an isothermal device due to waste heat rejection requirements. Therefor quantitative prediction of the effect of temperature on conductivity (power density), and on the EDB (efficiency) is required to assess the useful operating temperature range of this new fuel cell electrolyte. Secondly, analysis of the change in the electronic conductivity with temperature can help us understand the mechanism by which the dopant lowers the EDB.

The activation energy of the ionic conduction (Ei) was determined by measuring the conductivity at a PO_2 of 0.1 atm and plotting σT vs $10^3/T$, (σ = conductivity). The plot for Oxide B3 is shown in Figure 5. The slope yields an activation energy of 0.73 eV. This is in good agreement with the value of 0.69 eV calculated for $Ce_{0.8}Gd_{0.2}O_{2-Y}$ from the data in Figure 6 of reference (3). This indicates that the dopant is not altering the conduction of $O^=$ in the ceria lattice.

The impact of temperature on electronic conductivity was determined by measuring the total conductivity as a function of PO_2 at three temperatures. The ionic conductivity was then subtracted to yield σ_{el} vs PO_2 at the three temperatures. This data is shown in Figure 6. Best fit lines of slope = - 1/4 were drawn through the data at each temperature. Extrapolation to $PO_2 = 10^{-18}$ yielded σ_{el} as a function of temperature at a fixed PO_2. This data plotted as σT vs $10^3/T$ is shown in Figure 7, and yields an activation energy of 2.18 eV.

As pointed out by Kudo and Obayashi(3), this activation energy includes the enthalpy of reduction of the ceria lattice to generate the electrons as well as the activation energy for the mobility of the electrons (E_e). However since $E_e << E_i$, and E_i = 0.73 eV, the measured activation energy is dominated by the enthalpy of reduction term. In fact if one calculates the enthalpy of reduction per electron from Figure 7 of reference (3) for the composition $Ce_{0.8}Gd_{0.2}O_{2-Y}$ one obtains a very similar value of 2.17 eV. This indicates that the A dopant has not stabilized the ceria lattice against reduction, but more likely has reduced the number of electronic carriers by trapping electrons at the A sites in agreement with the original hypotheses.

The data in Figure 6 also yields EDB vs temperature by noting the PO_2 at which the electronic conductivity intersects the ionic conductivity value (marked by cross bars in Figure 6). Figure 8 shows the EDB plotted vs $10^3/T$ for B3 from this work, and compares it to $Ce_{0.8}Gd_{0.2}O_{2-Y}$ from reference (3). This illustrates that the nearly two orders of magnitude improvement in EDB holds over the whole temperature range of interest to fuel cells. The value of the EDB at 700°C taken from the least squares fit of this data is $3.7x10^{-21}$ for Oxide B3 vs $1.24x10^{-19}$ for $Ce_{0.8}Gd_{0.2}O_{2-Y}$ from the data of Kudo and Obayashi (3).

Figure 8 also provides insight into the upper temperature limit for useful fuel cell operation. Higher temperatures improve power density, but limit efficiency due to the increasing EDB. This data will be useful in predicting ceria cell performance as a function of temperature, and fuel composition.

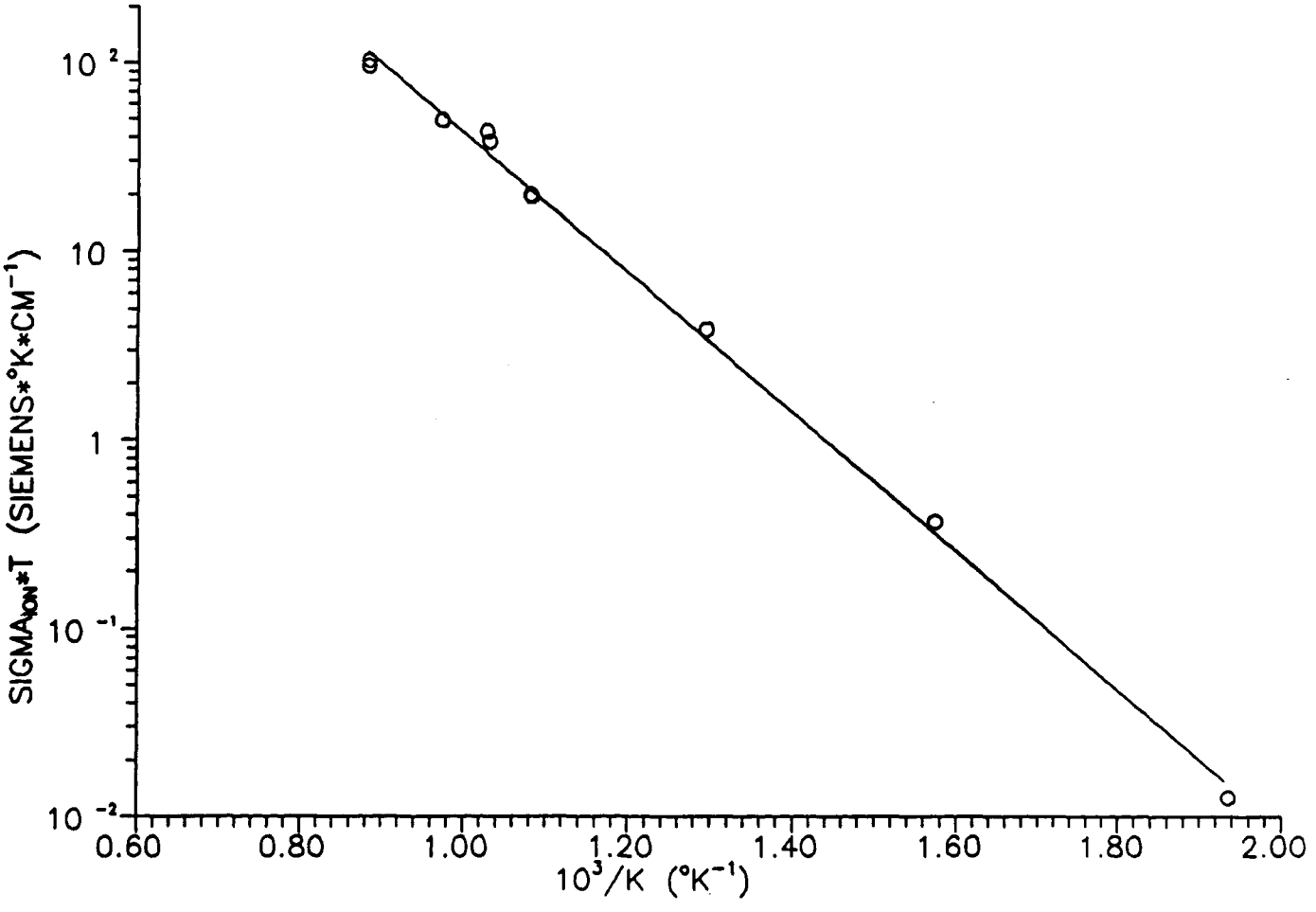

Figure 5. Ionic Conductivity – Temperature Behavior
Oxide B3 at $PO_2 = 10^{-1}$

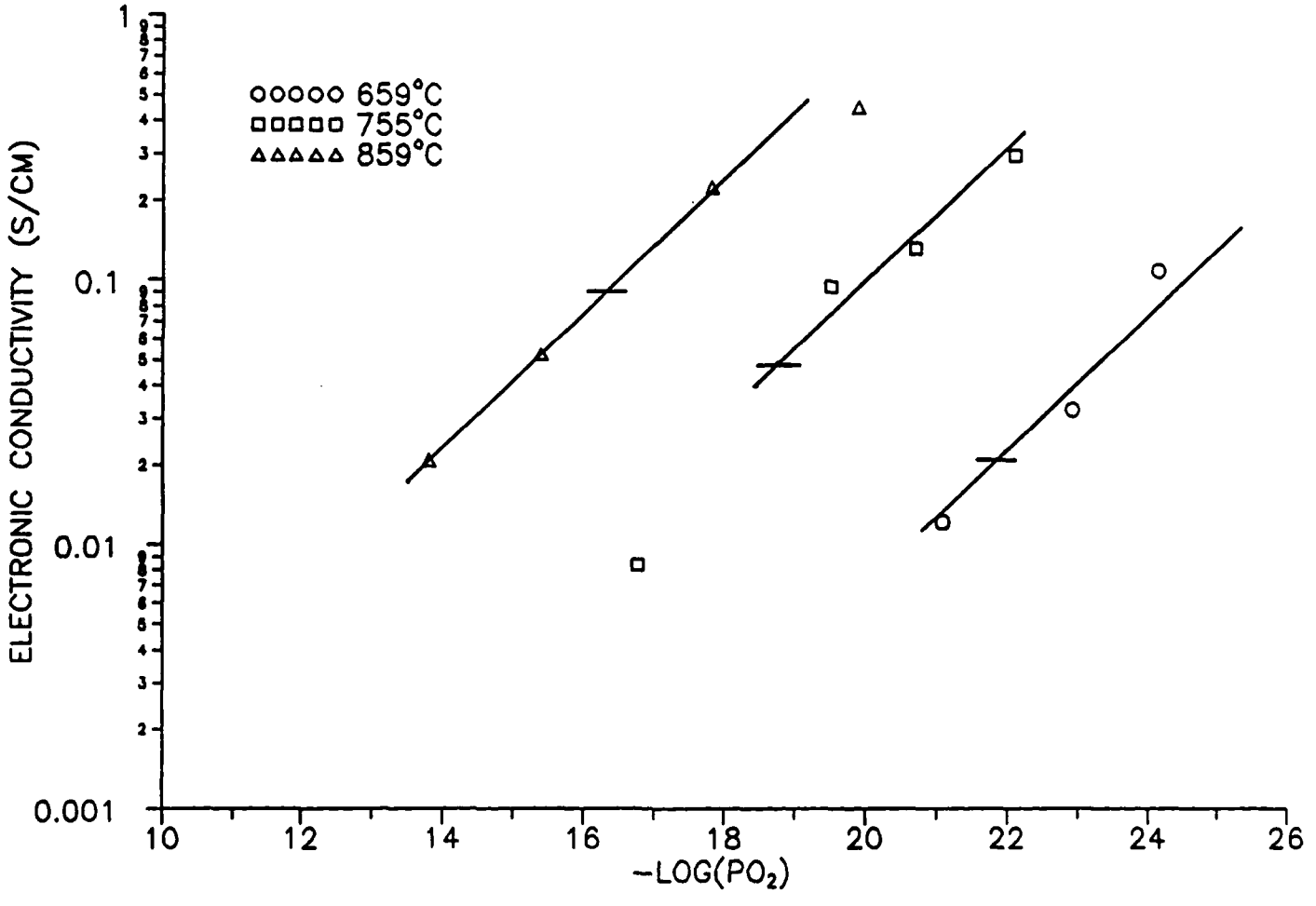

Figure 6. Electric Conductivity Vs. PO_2 at 3 Temperatures Oxide B3

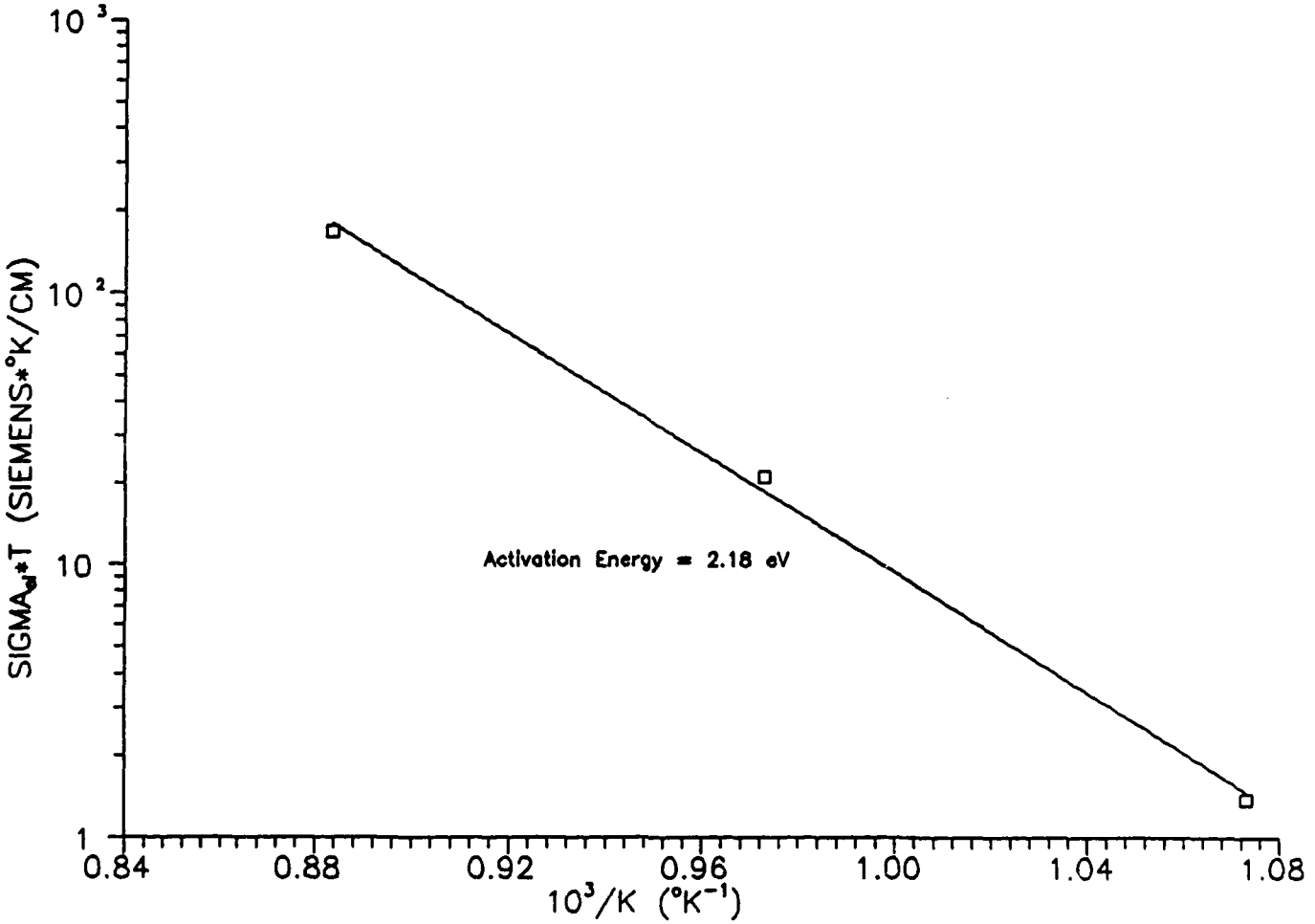

Figure 7. Electronic Conductivity - Temperature Behavior Oxide B3 at $PO_2 = 10^{-18}$

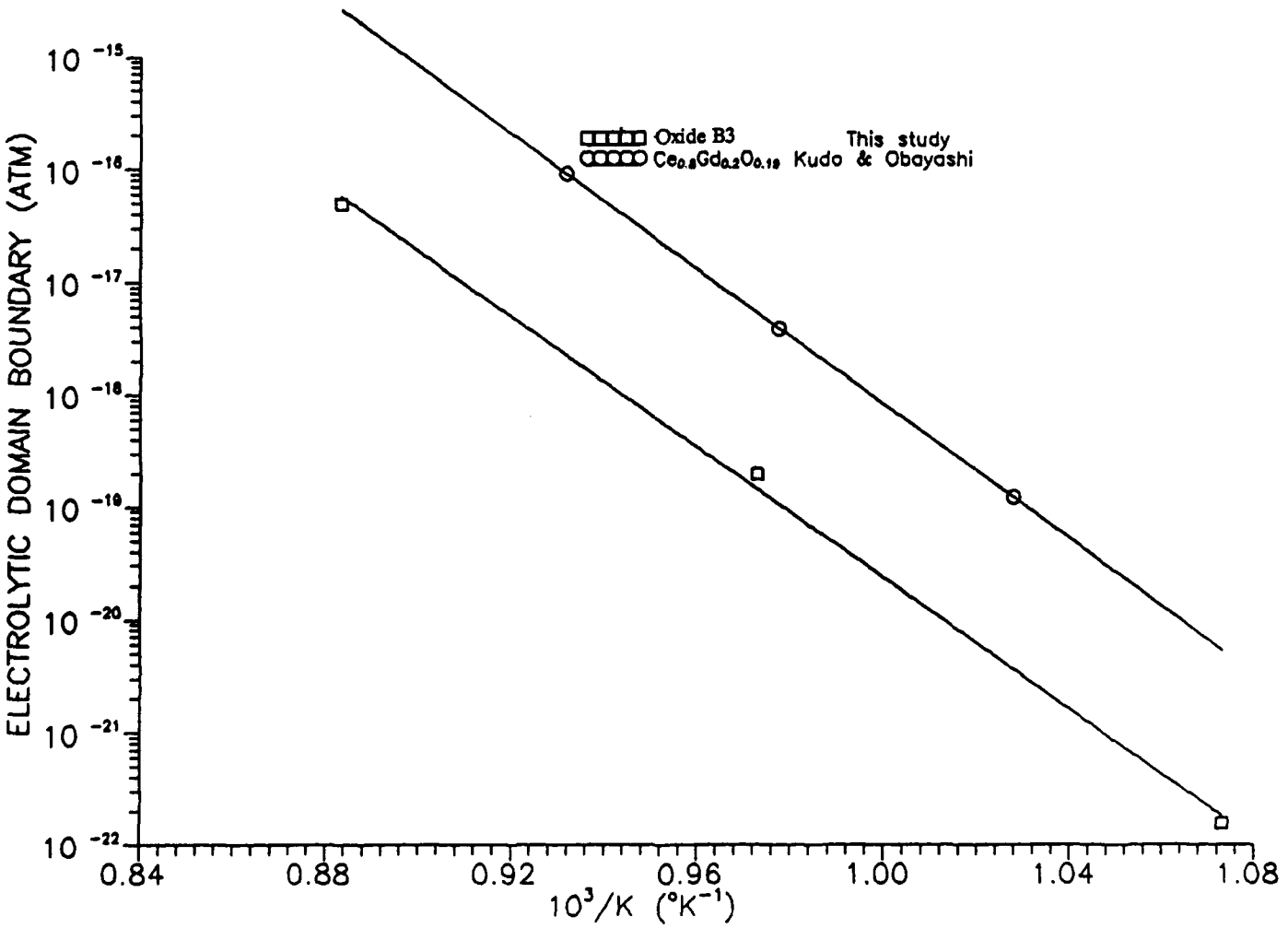

Figure 8. Temperature Behavior of Electrolytic Domain Boundary

2.5 Analysis of Bulk and Grain Boundary Conductivities as a Function of Temperature

A major advantage of using AC impedance analysis for the study of solid state electrolytes is the opportunity to separate grain boundary from bulk resistances. An operating fuel cell must contend with both sources of polarization losses. However, understanding the fundamental causes often leads to opportunities for engineering the material to optimize performance. In this case the bulk conductivity is a basic material property, but the grain boundary conductivity is determined by micro-structure and grain boundary chemistry (6). These are influenced primarily by processing parameters, and are therefor amenable to improvement by changes in processing technique. Separation of these two sources of iR losses is important in order to assess how much more improvement in the electrical properties of the doped ceria might be possible.

Increasing the ionic conductivity has a dual benefit. It improves the potential power density at a given electrolyte thickness, and at a fixed electronic conductivity vs PO_2 relationship, it lowers the EDB, improving efficiency. This provides strong incentive for determining if grain boundary resistance contributes substantially to overall electrolyte resistance.

In order to separate the grain boundary from the bulk impedance within the frequency range available from the Solartron 1250 FRA, it was necessary to lower the temperature well below 700°C. At temperatures in the 200 - 300°C range, two additional arcs are seen on the complex plane impedance plot (see Figure 1). Both lie between the lower end of the electrode curve and 0 on the real axis. The intersection of the upper end of the lowest arc on the real axis is assigned to the bulk, or lattice resistance, while the width of the intermediate arc on the real axis measures the grain boundary resistance (4)(5).

This technique was used to measure the bulk and grain boundary conductivities of several A doped ceria samples as a function of temperature. For reference $Ce_{0.8}Gd_{0.2}O_{2-Y}$ was included also. Figure 9 shows an example of conductivity plotted vs. $10^3/T$ for $Ce_{0.8}Gd_{0.2}O_{2-Y}$. Table III presents the bulk and grain boundary conductivities extrapolated to 700°C and the activation energies deduced from plots of σT vs $10^3/T$. Figure 10 illustrates this type of plot for Oxide B1.

TABLE III
BULK AND GRAIN BOUNDARY CONDUCTIVITIES
700°C, PO_2 = 0.1

Compound	σ_{Bulk} (S/cm)	σ_{Gb} (S/cm)	E_{Bulk} eV	E_{Gb} eV
$Ce_{0.8}Gd_{0.2}O_{2-Y}$	$1.5x10^{-1}$	$9.9x10^{-2}$	1.05	1.16
Oxide B1	$1.4x10^{-1}$	$6.9x10^{-2}$	0.92	1.02
Oxide B3	$3.4x10^{-1}$	*	0.90	*
Oxide B6	$1.04x10^{-1}$	$9.9x10^{-1}$	0.80	0.98

* Insufficient data

Inspection of the data in Table III reveals that the bulk conductivity of the B type samples is approximately twice the grain boundary conductivity. This means the grain boundary resistance is limiting the overall ionic conductivity, and substantial gains in ionic conductivity, and reduction of the EDB should result when the micro-structure is improved to minimize grain boundary resistance.

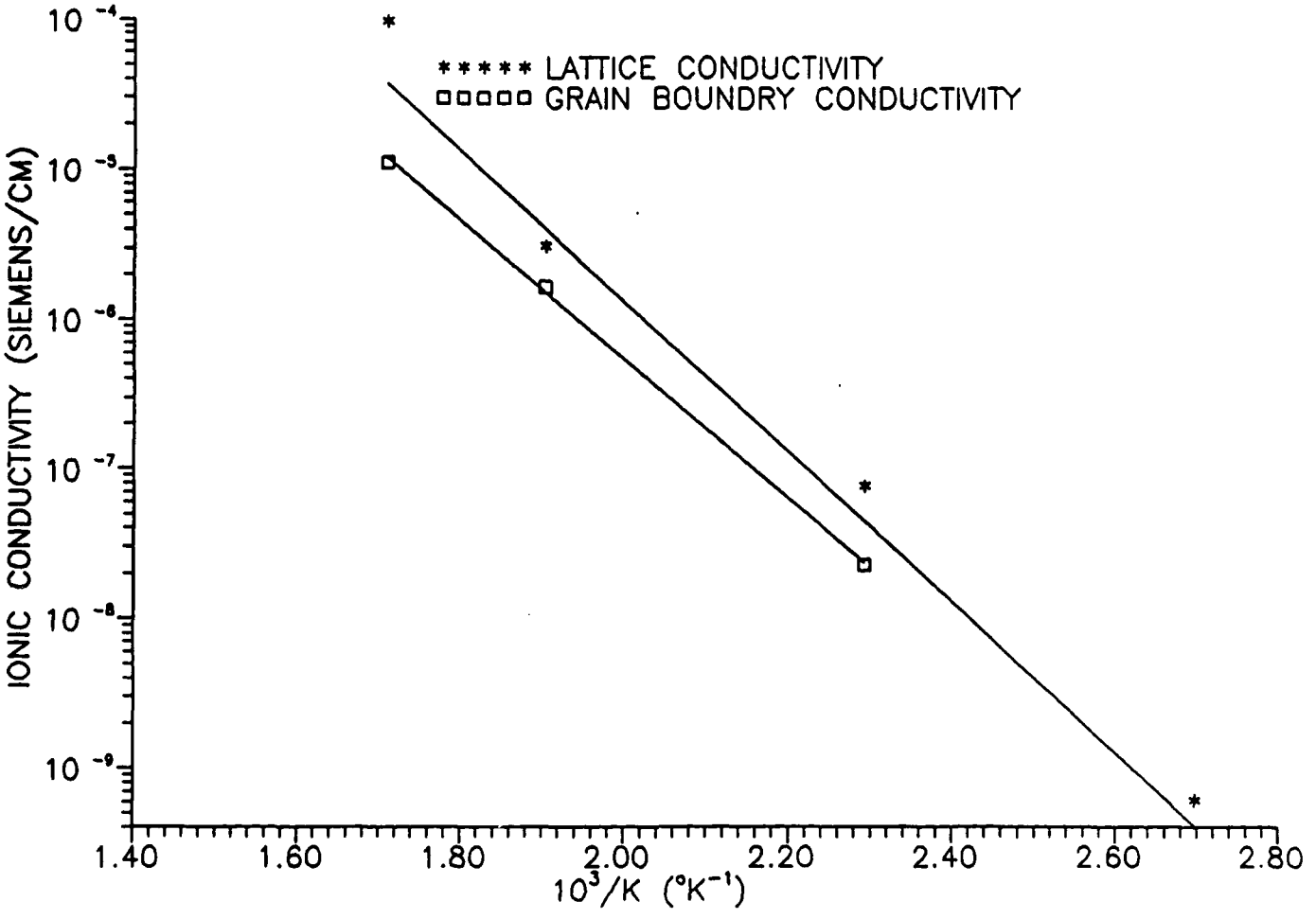

Figure 9. Conductivity Vs. Temperature, $PO_2 = 0.1$
$Ce_{0.8}Gd_{0.2}O_{2-Y}$

2.6 Impact of Grain Size on Electronic and Ionic Conductivity

In order to use a ceria as a practical fuel cell electrolyte, a density high enough to ensure no reactant cross leakage is required. Densities of the samples tested up to this point in the program ranged from 85-90 percent of theoretical. This is not high enough to ensure no through porosity. One approach to improving density is to use a high surface area, and therefor more sinterable starting material. This was accomplished by starting the mixed oxide synthesis with Opaline, a naturally occurring ceria available from Rhone Poulenc. This material has a relatively uniform particle size which lies mostly below 1μ

Discs prepared from Opaline did achieve an increase in density, to 93 percent of theoretical. However, when the electrical properties were measured this was found to be at the expense of ionic conductivity. The data is shown in Table IV.

TABLE IV
ELECTRICAL PROPERTIES OF B7
MADE FROM <1μ CERIA. 700°C

σion $PO_2 = 0.1$ (S/cm)	σel $PO_2 = 10^{-23}$ (S/cm)	EDB (atm)
2.5×10^{-2}	1.14×10^{-1}	4.5×10^{-21}

Both the ionic and electronic conductivities are lower by a factor of 2 then the data for B7 made from the 99.999 percent oxides with larger particle size. The smaller grain size which led to higher density also reduced the conductivities. Although the EDB is unchanged, the lower conductivity would adversely affect the potential fuel cell power density. This approach to improving density was not pursued.

2.7 New Compositions

It is of interest to know whether Dopant A is the only or even the most effective dopant. Other elements have similar properties and might perform the same function. Dopant B is a candidate. A sample of Oxide B5 was prepared and subjected to electrical evaluation. The data shown in table V illustrates that B produces the same reduction in EDB as A.

TABLE V
ELECTRICAL PROPERTIES OF OXIDE B5
At 700°C

σ_{ion} $PO_2 = 0.1$ (S/cm)	σ_{el} $PO_2 = 10^{-23}$ (S/cm)	EDB $PO_2 = 0.1$ (atm)	σ_{Bulk} $PO_2 = 0.1$ (S/cm)	σ_{Gb} (S/cm)
4.3×10^{-2}	1.7×10^{-1}	2.6×10^{-21}	1.88×10^{-1}	4.8×10^{-2}

Figure 11 shows the bulk, and grain boundary conductivities plotted vs temperature. The activation energies obtained from the σT plots were 0.94 eV and 0.93 eV for the lattice and grain boundary conductivities respectively.

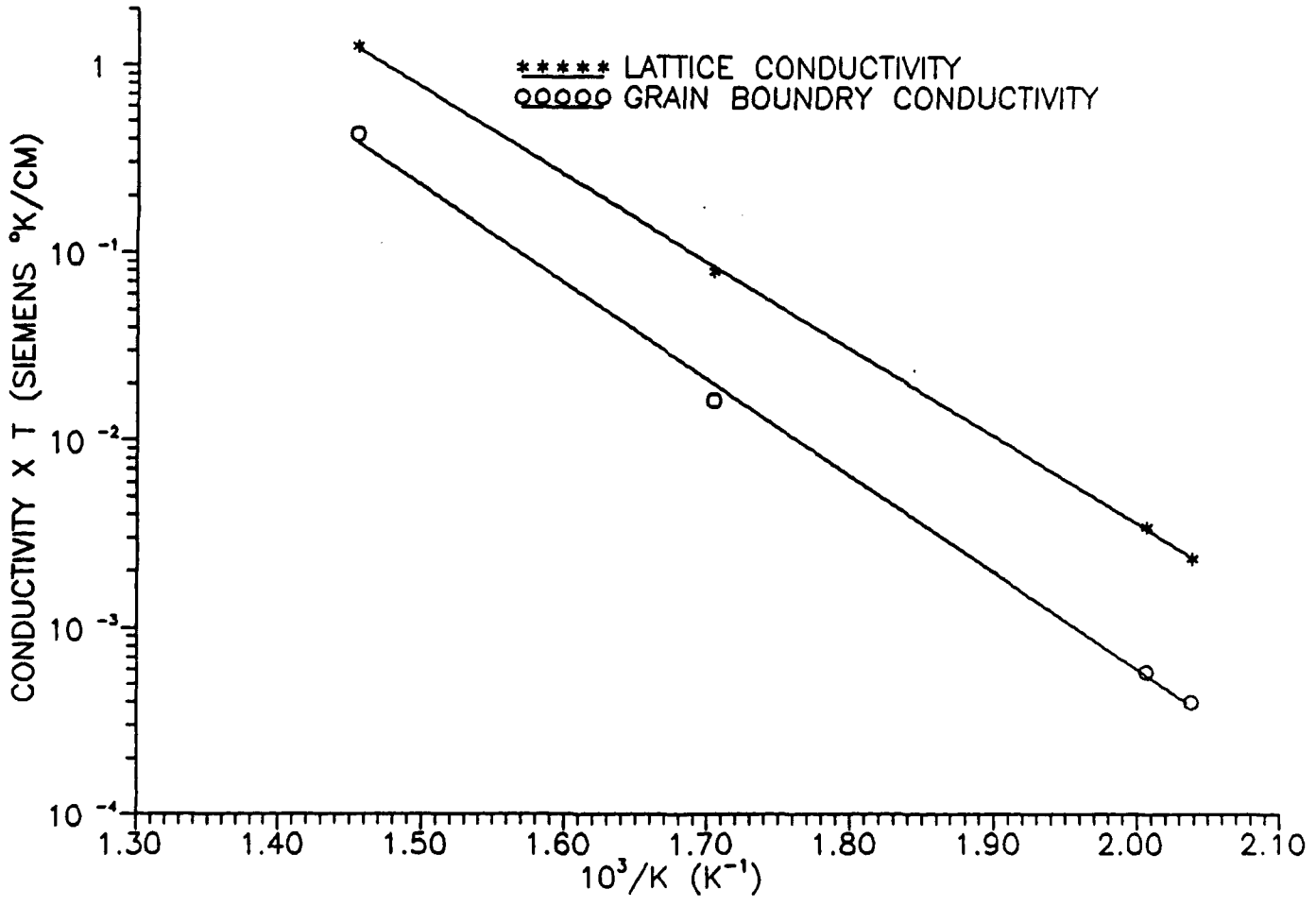

Figure 10. Conductivity *T Vs. Temperature, PO_2 = 0.1
Oxide B1

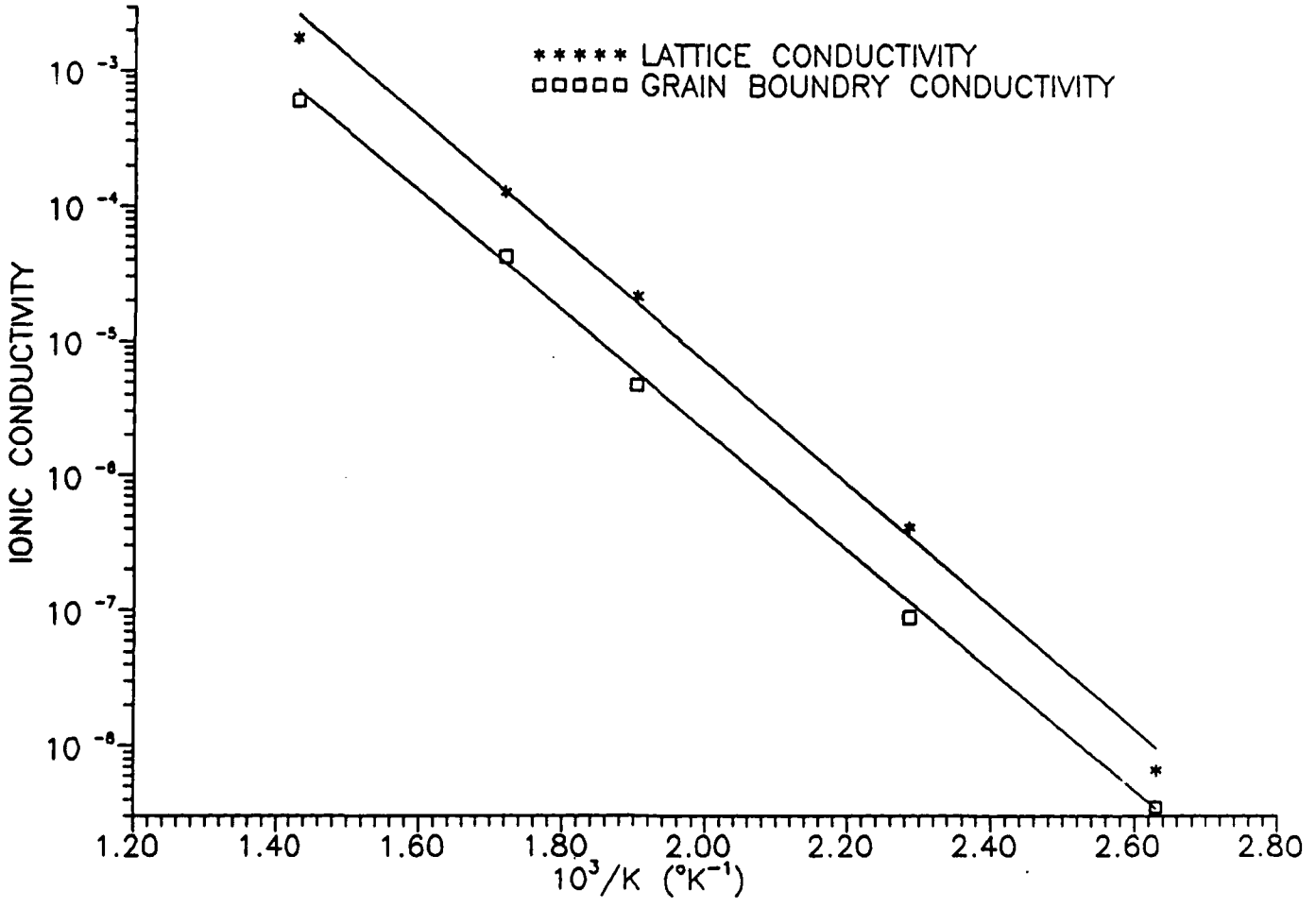

Figure 11. Conductivity Vs. Temperature, PO_2 = 0.1
Oxide B5

Task 3 Experimental Evaluation of Barrier Layers to Increase the Ratio of Ionic to Electronic Conductivity

3.1 Evaluation of Zirconia as Grain Boundary Barrier Layer.

Task 3 of this program proposed an alternative approach for lowering the EDB of ceria based electrolytes. This "barrier layer" concept involved introducing a grain boundary phase which had as high as possible ionic conductivity at 700°C, but no appreciable electronic conductivity. This was viewed as a fall back approach due to the expected ionic conductivity penalty.

A single attempt was made to test this concept based on a gel coating process developed by Prof. Samantha Amarakoon of Alfred University (7)(8). A sample of Oxide B1 powder was sent to Alfred University, where it was gel coated with yttria stabilized zirconia. This produced a two phase powder with an electronically insulating coating around a core of doped ceria. Analysis at IFC revealed a ZrO_2 level of 1.3 wt percent. This material was then processed into a disc as described in Section 2.1. No changes were made in the sinter cycle since densities were already low. The plan was to leave the ZrO_2 as a grain boundary phase, providing a barrier to electronic conduction. Electrical properties are shown in Table VI.

TABLE VI
ELECTRICAL PROPERTIES OF OXIDE B1
FABRICATED FROM ZrO_2 COATED POWDERS
700°C

σ_{ion} $PO_2 = 0.1$ (S/cm)	σ_{el} $PO_2 = 10^{-23}$ (S/cm)	EDB (atm)	σ_{Bulk} $PO_2 = 0.1$ (S/cm)	σ_{Gb} $PO_2 = 0.1$ (S/cm)
3.0×10^{-2}	1.62×10^{-1}	1.1×10^{-20}	7.8×10^{-2}	1.15×10^{-1}

Comparison of this data with Table III reveals that the net result of adding the ZrO_2 was to lower the ionic conductivity while leaving the electronic conductivity almost the same. This raised the EDB, the opposite of the desired result.

Figure 12 shows the grain boundary and bulk conductivities vs temperature data for this sample. The extrapolated 700°C conductivities (Table VI) compared to the uncoated sample of the same composition (Table III) show lower bulk conductivity and higher grain boundary conductivity. This is just the reverse of the expected result if the ZrO_2 were a grain boundary phase. The implication is that the Zr diffused into the ceria during the sinter cycle, lowering the bulk ionic conductivity. A sintered sample has been returned to Alfred University for verification of this conclusion by transmission electron microscopy.

The ZrO_2 did however perform the roll of a sintering aid. This led to a high density (93% of theoretical) which presumably helped improve the grain boundary conductivity. The activation energies from σT vs $10^3/T$ analysis were 0.98 eV, and 0.88 eV for grain boundary and bulk conductivities respectively.

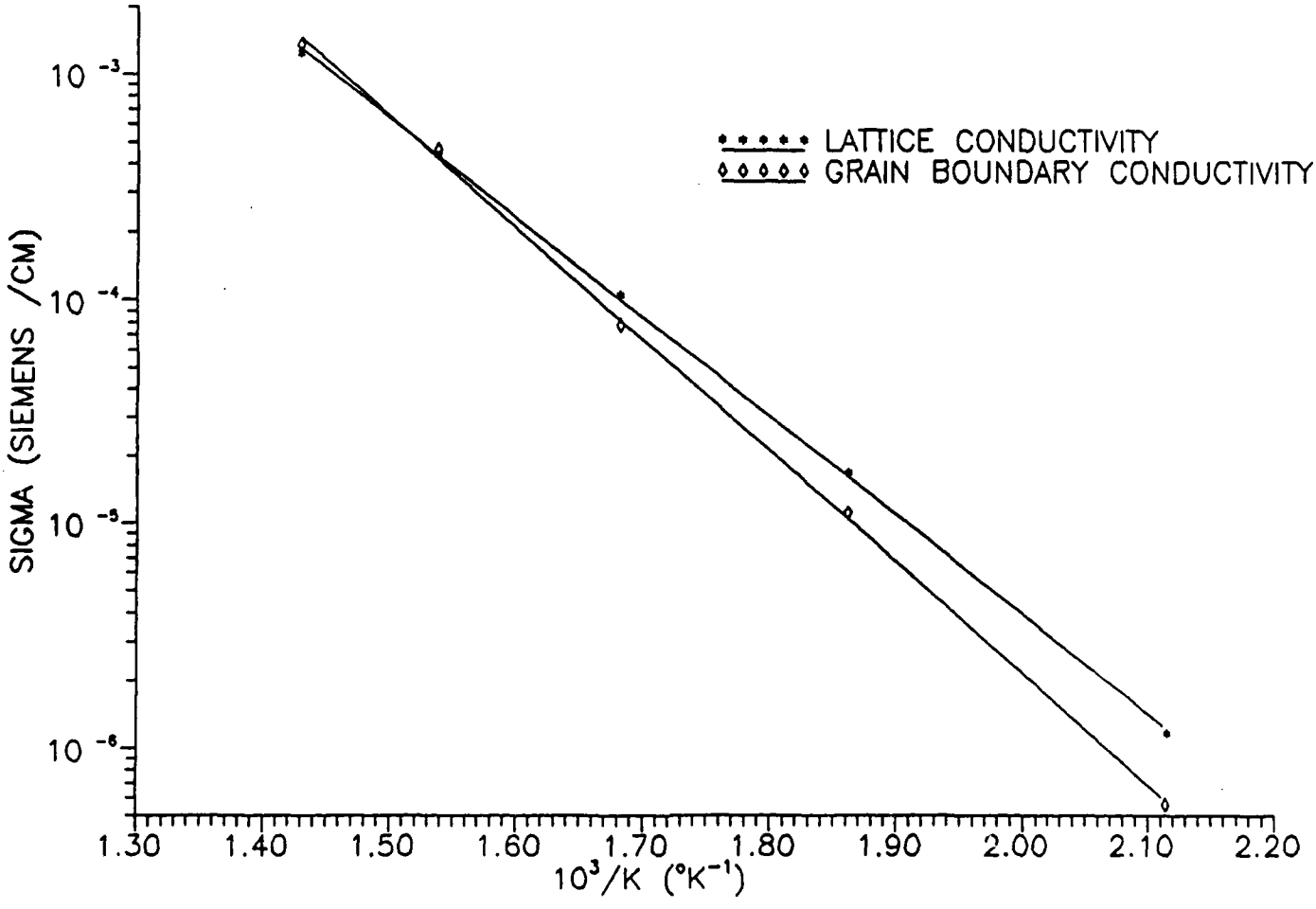

Figure 12. Conductivity Vs. Temperature PO_2 = 0.1 ATM Oxide B1 From ZrO_2 Gel Coated Powder

On the basis of this experience, the doping concept rather than the barrier layer was selected as the approach to pursue in Phase II of this program. This decision reflected primarily the perceived difficulty of achieving phase separation and density at the same time with a practical fabrication process.

Phase I Program Review

A. Recommended Approach

At the request of the DARPA Program Manager, a rough development plan leading to a 1-kW demonstration of this technology was prepared. The plan is presented in Appendix A.

REFERENCES

(1) "Conduction in Heterogeneous Systems," Meredith, R. E., and Tobias, C. W., in Advances in Electrochemistry and Electrochemical Engineering, Tobias and Delahay ed, Vol 2, Interscience Publishers, (1962) pp 15 - 45.

(2) Tuller, H. L., and Nowick, J. Electrochem. Soc., 122 No 2 pp 255-259, (1975).

(3) Kudo, T., and Obayashi, J. Electrochem. Soc., 123 No 3 pp 415-419, (1976)

(4) Wang, D., Y., and Nowick A., S., J. Solid State Chem. 35 pp 325-333, (1980)

(5) Gerhardt, R., and Nowick, A., S., J. Am. Ceram. Soc., 69 pp 641-646, (1986)

(6) Gerhardt et al. J. Am. Ceram. Soc. 69 pp 647-651, 1986

(7) Selmi, F. A., and Amarakoon, V. R. W., J. Am. Ceram Soc. 71 pp 943-937, (1988)

(8) Selmi, F. A., and Amarakoon, V. R. W., Ceramic Engineering and Science Proceedings 8 September-October, (1987)

DISTRIBUTION LIST

Director
Advanced Research Project Agency
1400 Wilson Boulevard
Arlington, Virginia 22209
Attn. Dr. David Squire
(2 Copies)

Administrative Contracting Officer
DCASMA-Hartford
96 Murphy Road
Hartford, CT 06114-2173
(1 copy)

Defense Technical Information Center
Bldg. 5, Cameron Station
Alexandria, Virginia 22314
(2 Copies)

Director
Naval Research Laboratory
Attn. Code 2627
Washington, D. C. 20375
(1 Copy)

APPENDIX A

APPENDIX A

CERIA CELL CONCEPT

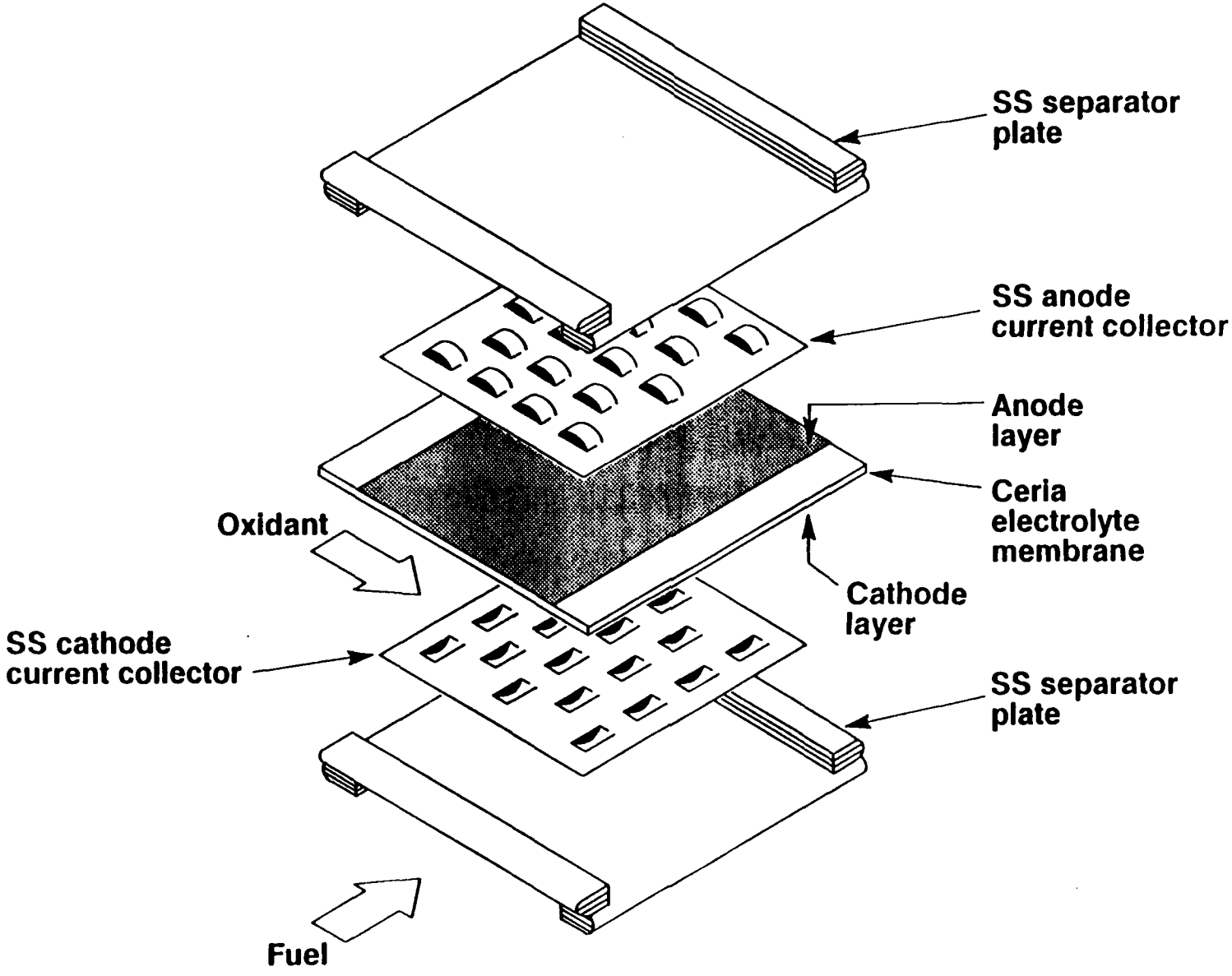

CERIA ELECTROLYTE DEVELOPMENT PLAN

- PHASE I – 18 MONTHS, ENDED DECEMBER 1989
  - DEVELOPED ELECTROLYTE COMPOSITION WHICH LOWERED ELECTRONIC SHORT TO ACCEPTABLE LEVELS

- FISCAL 1990 PROGRAM
  - DEVELOP THIN ELECTROLYTE DISC
  - DEVELOP CATHODE
  - TEST DISC CELL

- FISCAL 1991 PROGRAM 12 MO
  - OPTIMIZE ANODE
  - SCALE UP & FAB PARTS FOR 1KW–SCALE SINGLE CELL TEST
  - DESIGN SHEET METAL PARTS
  - DEVELOP SEALS
  - TEST 1 KW–SCALE SINGLE CELL

- FISCAL '92 – '93 1 KW–STACK PROGRAM
  - STACK DESIGN
  - REPEAT PART PROCESS DEVELOPMENT
  - FABRICATION
  - TEST

1990 CERIA PROGRAM PLAN

- TASK I ELECTROLYTE DEVELOPMENT AND FABRICATION
  - DEVELOP FABRICATION PROCESSES
  - FABRICATE ELECTROLYTES FOR TASKS II AND III

- TASK II DEVELOP A CATHODE FOR THE CERIA CELL
  - PROCURE CANDIDATE MATERIALS
    - –NIOBIUM DOPED CERIA
    - –STRONTIUM DOPED LANTHANUM MANGANATE
  - DEVELOP SLURRY CAST APPLICATION TECHNIQUE
  - FABRICATE CATHODES FOR TESTING

- TASK III CELL TEST CATHODES
  - DEVELOP CERIA DISC CELL SEAL
  - APPLY NI/ZIRCONIA ANODE
  - TEST DISC CELL
  - FINAL REPORT DOCUMENTING ELECTROLYTE FABRICATION AND CATHODE DEVELOPMENT

ONR/DARPA CERIA PROGRAM
1990 PROGRAM PLAN

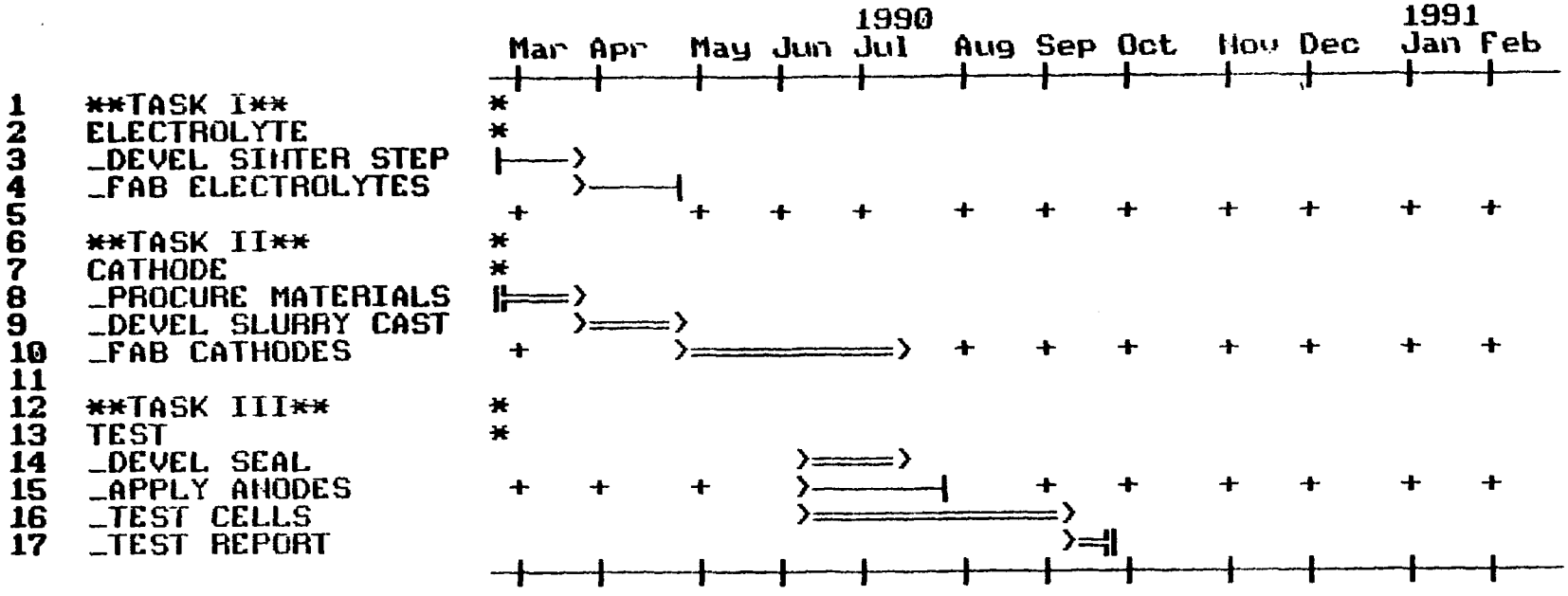

1991 CERIA PROGRAM PLAN

- TASK I OPTIMIZE ANODE FOR CERIA CELL
  - SELECT CANDIDATE MATERIALS
    - –UNDOPED CERIA
    - –NICKEL ZIRCONIA CERMET
  - DEVELOP FABRICATION TECHNIQUE
  - TEST DISC CELL

- TASK II SCALE UP & FAB PARTS FOR 1KW SIZE CELL
  - ELECTROLYTES (NOMINAL 5x5 INCHES)
  - ANODES
  - CATHODES
  - SHEET METAL HARDWARE

- TASK III DESIGN SHEET METAL SINGLE CELL COMPONENTS
  - CANDIDATE MATERIALS AND CONFIGURATIONS DERIVED FROM MOLTEN CARBONATE TECHNOLOGY

- TASK IV DEVELOP SEALS
  - CELL EDGE SEALS
  - STACK GAS MANIFOLD SEALS
  - CANDIDATE SEALS FROM MOLTEN CARBONATE TECHNOLOGY

- TASK V RUN 1KW SIZE SINGLE CELL TESTS
  - ASSEMBLE TEST CELLS
  - TEST

ONR/DARPA CERIA PROGRAM
1991 PROGRAM PLAN

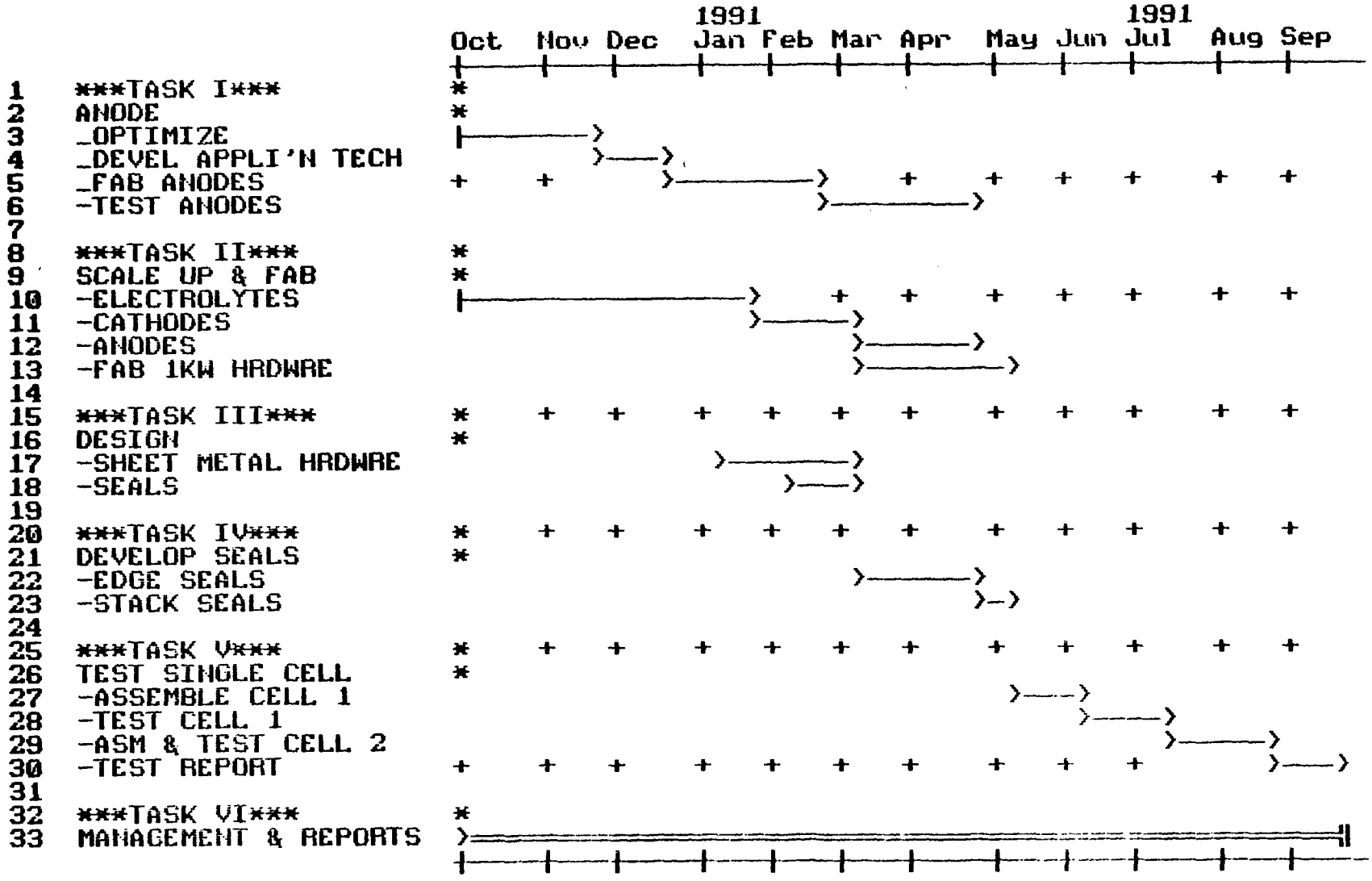

1 KW-STACK CERIA PROGRAM PLAN

- TASK I DESIGN STACK
  - CELL PACKAGE (ANODE/ELECTROLYTE/CATHODE)
  - SHEET METAL CURRENT COLLECTORS
  - SEPARATOR PLATES
  - SEALS

- TASK II REPEAT PART PROCESS DEVELOPMENT
  - CELL PACKAGE
  - SHEET METAL

- TASK III FABRICATION - 50 CELLS
  - CELL PACKAGE
  - CURRENT COLLECTORS
  - PLATES
  - SEALS
  - NON-REPEAT STACK HARDWARE

- TASK IV 1-KW CERIA STACK TEST
  - MODIFY TEST STAND
  - STACK ASSEMBLY
  - STACK TEST
- TASK V MANAGEMENT AND REPORTING

1 KW CERIA STACK PROGRAM PLAN
1992 - 1993